



## **Mapping and modelling a boreal forest soil organic carbon predictor in the glacial till of Newfoundland, Canada**

Scout M. Quinn<sup>1,2</sup>, Benjamin Misiuk<sup>1,2</sup>, Mackenzie E. Patrick<sup>1,†</sup>, Susan E. Ziegler<sup>1</sup>

<sup>1</sup>Department of Earth Sciences, Memorial University of Newfoundland and Labrador, St John's, A1C 5S7, Canada

<sup>2</sup>Department of Geography, Memorial University of Newfoundland and Labrador, St John's, A1C 5S7, Canada

5 † Deceased

Correspondence to: [smquinn@mun.ca](mailto:smquinn@mun.ca)



## Abstract

Boreal forest soils store 30% of global forest soil carbon, making them a crucial component of the carbon cycle. However, climate change at high latitudes is resulting in heightened temperatures and increasingly unpredictable precipitation patterns. Soil organic carbon (SOC) formation and stabilization is tied to precipitation patterns, thus climate change will inevitably influence the stability and longevity of boreal forest SOC. The current size and distribution of this reservoir is poorly understood, creating uncertainty under current and future climate scenarios. Previous research demonstrates mineral soil properties may be used to model boreal forest SOC accurately. The surface slope, depth of carbon enriched horizon, and climate characteristics are important parameters for modelling SOC and can generally be obtained or estimated via remote sensing. However, information about aluminum availability – the weatherable aluminum capable of interacting with organic matter to form stable carbon rich organometal complexes in mineral soils – is not widely available but is controlled by soil parent material. To bridge this gap, the Newfoundland and Labrador till geochemistry dataset was used here to map and model aluminum availability in glacial till across the island of Newfoundland as a function of geology and climate. The Random Forest Algorithm was employed to develop two models: one relying solely on the strength of geological and climatic variables, and the other drawing additionally on the spatial context of sample points. The first model performed well ( $R^2=0.60$ ), however, adding a spatial component increased the performance of the second model ( $R^2=0.71$ ). Bedrock type and proximity of the samples to certain units were indicated to be the strongest controls on aluminum availability, while environmental factors were less influential. Additionally, model uncertainty was calibrated empirically and mapped spatially, providing reliable and actionable information about the confidence of predictions over the study area. This project demonstrates the value of predictive geospatial modelling for till geochemistry mapping and delivers key aluminum availability predictions for deriving SOC reservoir estimates across Newfoundland.



## 1 Introduction

30 Soils are a crucial component of the global carbon cycle, with soil carbon (C) stocks on average three times larger than the atmospheric C reservoir (Scharlemann et al., 2014). Of this, boreal forest soils store 30% of global forest soil C alone (Scharlemann et al., 2014). This is primarily stored in podzols – an acidic mineral soil characterised by a nutrient- and organic-depleted eluvial (Ae) horizon overlying the enriched illuvial (B) horizon (Hagemann et al., 2010). Soil organic carbon (SOC) is sequestered when dissolved organic matter leached from the overlaying organic layer infiltrates into the mineral soil and  
 35 interacts with reactive metals, precipitating as organometal complexes (OMCs) in an organic matter enriched soil horizon (Baldock & Skjemsted, 2000). Transport of SOC through the soil profile to the persistent deep mineral soil C pool depends on water infiltration, with SOC stabilisation influenced by climate regulated microbial composition and activity (Jackson et al., 2017; Wang et al., 2022). Soil C storage potential in boreal forests is linked to a variety of soil parameters such as texture, clay content, acidity, cation availability, and environmental factors such as climate, topography, and parent material (Oades, 1988;  
 40 Slessarev et al., 2022; Patrick, 2023). However, in these young soils, mineralogical controls, dominated by reactive Al availability (Patrick et al., 2022), are one of the strongest predictors of SOC (Rasmussen et al., 2018).

Amplified climate change in high latitudes raises concerns about vulnerable boreal SOC stocks as the current and future size and distribution of this reservoir under various climate scenarios are poorly constrained, introducing uncertainty in models relying upon such estimates (Crowther et al., 2016; Friedlingstein et al., 2014; Wang et al., 2022). Consequently, unravelling  
 45 climate-SOC feedback loops is crucial to predict the SOC stock evolution under future climate scenarios (Friedlingstein et al., 2014; Jackson et al., 2017). Additionally, evaluating this reservoir at global, regional, and local scales is key to mitigating climate change. Land use and resource extraction management can mitigate terrestrial CO<sub>2</sub> loss into atmospheric or aquatic reservoirs (Wang, 2020). Such practices include modifying agricultural techniques to include low tillage practices and fertilizer amendments, or reforestation and harvesting plans that encourage SOC retention (Ameray et al., 2021; Hillier et al., 2012).

50 Friedlingstein et al. (2014) analysed SOC estimates from 11 participants in the 5th Climate Model Intercomparison Project and found estimates ranged from 510 to greater than 3000 Pg, with wide error margins disproportionately affecting high latitude regions. This is because SOC is modelled globally using earth system models (ESMs), which synthesize results of smaller models to provide insight into environmental context, climatic conditions, and soil properties (Pierson et al., 2022). Podzol-specific SOC storage mechanisms are often not incorporated into such models, and boreal regions are thus poorly modelled –  
 55 likely a consequence of low sample density in high latitude areas (Pare et al., 2024). For example, productivity attributes often dictate SOC predictions (Zhang et al., 2020), however these are unreliable at high latitudes where organic input is scant and undergoes protracted decomposition due to low temperatures and elevated acidity (Pare et al., 2024; Zhou et al., 2024). Additionally, in some cases soil texture properties have been improperly positively related to SOC storage; the CENTURY climate model (Parton, 1993) associates higher clay fractions with increased SOC stocks, obscuring the importance of other  
 60 mineralogical controls (Patrick, 2023, Pare et al., 2024; Rasmussen et al., 2018; Zhang et al., 2020). Research suggests that a fine scale approach delivers higher accuracy and more realistic estimates over regional extents (Deluca & Boisvenue, 2012;



Jackson et al., 2017; McNicol et al., 2019; Pare et al., 2024; Pierson et al., 2022). For example, constraining models to the biome scale may normalize the effects of climate and illuminate SOC mechanisms that may otherwise be concealed (Patrick, 2023).

65 The C saturation of OMCs, the proportion of SOC in OMCs, and soil Al availability have been used to model soil C stocks in inaccessible, poorly sampled upland boreal forest soils on the Island of Newfoundland highlighting Al availability as a key predictor of SOC (Patrick 2023). Available Al refers to the proportion of total Al stored in reactive poorly crystalline minerals (PCMs) which form C-Al OMCs (Slessarev et al., 2022). The Al availability (Al%) is calculated via the chemical index of alteration (CIA) which compares the content of highly stationary Al oxides to more mobile Ca, Na, and K oxides (Nesbitt & 70 Young, 1984). Slope, depth of enriched horizon, and climate can be modelled to extrapolate saturation of OMCs and proportion of SOC within OMCs. However, soil Al% is not so easily estimated and is currently obtained through intensive field work and laboratory analyses. Assessing the controls influencing Al OMC precipitation is key to predicting SOC in these soils, and parent material (Patrick et al. 2022; Patrick 2023). Geological maps are often used as a proxy for parent material; however, this ignores the suitability of different lithologies to acquiesce more mineralogical material than others to soil forming 75 processes and explains little about the persistence of effects of parent material (Lawley & Smith, 2008). Unsurprisingly, surficial geology has been found to be a consistently significant control of SOC at local to regional scales (Adhikari et al., 2020). On the Island of Newfoundland, and in many boreal regions, parent material is dominantly glacial till, not bedrock, rendering it especially relevant to incorporate this dimension into SOC modelling. First mapping the till composition and using this to support a sampling design to capture a range of Al% in soils across a variety of slopes and climatic conditions would 80 provide a means to explore this parent material - Al OMC connection (Patrick 2023).

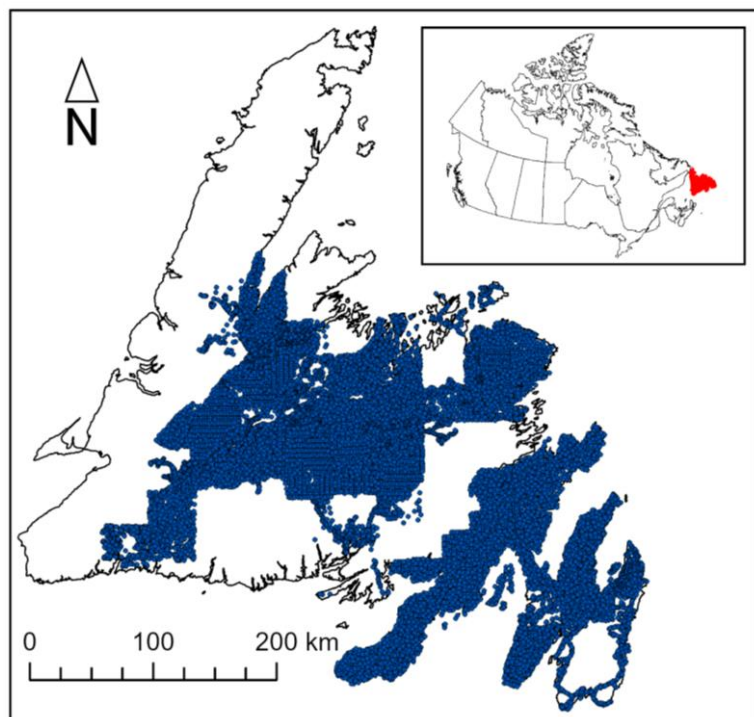
The aim of this paper is to create a high-resolution geospatial model predicting the distribution of Al rich weatherable minerals in glacial till in Newfoundland. This is a critical step toward attaining accurate regional estimates of boreal forest soil SOC stocks across the Island of Newfoundland. We model Al% spatially as a function of covariates believed to influence Al geochemistry. Because till geochemistry is controlled by geological parent material, and because Al is a relatively immobile 85 element, we hypothesise that bedrock geology will be the strongest predictor for Al%. Two models are trialled in this study: a highly specific spatial model using both environmental covariates and geographic location information, and a more general aspatial model relying solely on environmental covariates. We hypothesise that the spatial model may be useful in areas that have been extensively sampled and the aspatial version may have a higher capacity to extrapolate predictions to areas with fewer samples. Predictive maps of Al and calibrated spatial estimates of their uncertainty are produced as objectives of this 90 project. Calibration of predictive uncertainty is crucial for delivering accurate estimates of model confidence that can be used directly in future SOC modelling. These objectives will contribute to the establishment of a continuous spatial SOC stock estimate for the Island of Newfoundland.



## 2 Methods

### 2.1 Till dataset

95 Publicly available till geochemistry data was sourced from the Geological Survey of Newfoundland and Labrador (GSNL; GSNL, 2024). This dataset was developed from till surveys conducted by the GSNL between 1985 and 2023 and spans much of the island (see figure 1). The inconsistent sample distribution can be attributed to sampling primarily being conducted according to National Topographic System map sheets. Samples were collected 40-60 cm deep on average and were large enough to obtain ~0.50 kg of till matrix, with larger clasts discarded (GSNL, 2024). Samples were dried and sieved using  
 100 either a <180 µm or <63 µm sieve. Samples underwent gravimetric analysis and the remaining solid was digested in 15 ml of concentrated hydrofluoric acid, 5 ml of concentrated hydrochloric acid, and 5 ml of 50 volume percent HClO<sub>4</sub>. Further addition of concentrated 10% HCl was added if dissolution was not achieved. Geochemical composition of the solution was determined by the GSNL using inductively coupled plasma emission spectroscopy (ICP-OES). Results are given in wt% for elements of interest which were Na, Ca, K, and Al.



105 **Figure 1** Distribution of till geochemistry samples from the Geological Survey of Newfoundland and Labrador across Newfoundland



## 2.2 Covariates

Covariates were selected to represent geological setting (surficial geology, regional geology), landscape characteristics (slope, ruggedness, elevation), and environmental context (climate region, distance from ocean). Additionally, a second model was developed that included layers representing the distance to each bedrock unit to provide spatial context. This ensures the model will consider the relationship of till geochemistry to the immediate bedrock unit, and within the greater geological setting (Fig.2).

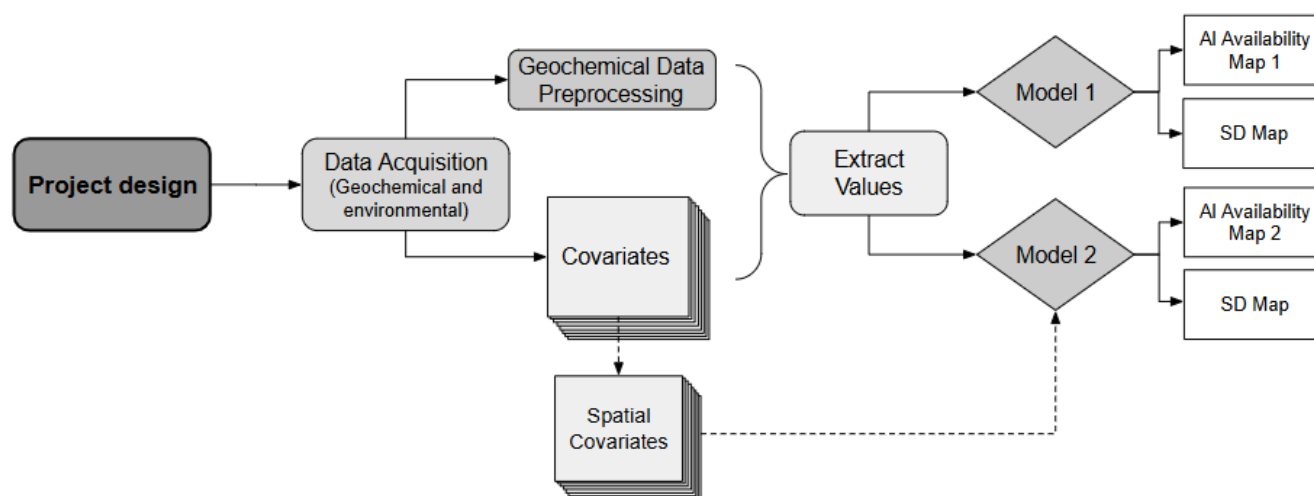


**Figure 2 Project workflow for aluminum availability (Al%) models 1 and 2 and their respective standard deviations (SD)**

## 2.3 Preprocessing

Till samples with Al, Na, Ca, and K values below the detection limit were removed, as were those with extremely low arbitrary values, which were identified as artefacts of the ICP OES analysis. Elemental composition was reported in terms of wt% oxide. To assess the degree of mineral weathering, the chemical index of alteration (CIA) (Nesbitt & Young, 1984) was calculated and compared to initial Al concentration values following Eq. (1):

$$CIA = \frac{Al_2O_3}{Al_2O_3 + CaO + K_2O + NaO} \times 100. \quad (1)$$

The Al% was then derived using Eq. (2):



$$Al\% = \frac{100 - CIA}{100} \times Al_2O_3 \times 100, \tag{2}$$

where Al% is expressed as a weight percent of oxides.

125 A set of environmental covariate rasters were developed to model Al% spatially (Table 1). GSNL data layers were  
all converted to rasters with a resolution of 20 m in ArcGIS Pro across the full extent of the Island of Newfoundland.  
Categorical variables were coded numerically for modelling (bedrock geology unit 1-46; surficial geology units 1-9; climate  
zones 1-7). The “Near” tool in ArcGIS Pro was used to obtain the distance from the coastline to the centre of each raster cell,  
represented as a point layer, which was rasterized to match the resolution and extent of the other layers. Mean monthly  
130 snowfall, evapotranspiration, and air temperature were acquired from the FLDAS Noah Land Surface Model at 0.1° resolution  
for the period 01/01/1982 to 30/04/2024 (McNally et al, 2018). The mean annual precipitation layer was derived from the  
WorldClim layer obtained from the ArcGIS Living Atlas at 3 km resolution (Fick & Hijmans, 2017). The data were masked  
to the study area, converted to vector format, and joined to one single 20 m grid-like polygon layer with an extent matching  
the raster layers. Values were interpolated in areas missing data using nearest neighbours within 10 km. This was done in  
135 preparation for use of the “Multivariate Clustering” tool in ArcGIS Pro, which was then used to identify seven climate zones  
using the mean annual precipitation and mean monthly snowfall, evapotranspiration, and air temperature values from the grid-  
like layer. The map of the climate zones was then converted to a raster. The NLDEM (GovNL, 2023) was used for elevation  
values. Although the NLDEM has a higher resolution, it comprises rounded integer values making the calculation of terrain  
attributes from this data source unsuitable. Therefore, slope and roughness were calculated from the Canada high resolution  
140 DEM (Government of Canada, 2024) in R using the MultiscaleDTM package (Ilich et al., 2023).

**Table 1 Characteristics and sources of the geospatial data layers used for model development. N/A indicates that these are not applicable to a given layer.**

| Layer                      | Original Resolution | Transformation                | Source     |
|----------------------------|---------------------|-------------------------------|------------|
| Till Geochemistry Dataset  | N/A                 | N/A                           | GSNL, 2024 |
| Regional Surficial Geology | 1:250,000           | Rasterize (20 m) <sup>a</sup> | GSNL, 2024 |
| Regional Bedrock Geology   | 1:1,000,000         | Rasterize (20 m) <sup>a</sup> | GSNL, 2024 |



|                           |             |  |                             |
|---------------------------|-------------|--|-----------------------------|
| Distance to Bedrock Unit  | 1:1,000,000 | Rasterize (20 m) <sup>a</sup><br>Calculate Euclidean Distance <sup>b</sup> | Modified from<br>GSNL, 2024 |
| Annual Precipitation      | 3 km        |  |                             |
| Annual Snowfall           | 0.10 degree | Multivariate Clustering,   | Fick & Hijmans,<br>2017     |
| Annual Temperature        | 0.10 degree | Rasterize (20 m) <sup>a</sup>  | McNally et al., 2018        |
| Annual Evapotranspiration | 0.10 degree |  |                             |
| Distance From Ocean       | 20 m        | Calculate Euclidean Distance <sup>b</sup>                                  | N/A                         |
| Elevation                 | 5 m         | Resample (20 m) <sup>b</sup>   | GovNL, 2023                 |
| Slope                     |             |  | Derived from                |
|                           | 16 m        | Resample (20 m) <sup>b</sup>   | Government of               |
| Ruggedness                |             |  | Canada, 2024                |

<sup>a</sup>resampling method: nearest neighbor, <sup>b</sup>resampling method: bilinear

145 Additional data layers were produced representing spatial and geological context of points. The Euclidean Distance tool in ArcGIS Pro was used to create layers indicating the nearest distance to each of the GSNL Regional Bedrock Geology units. This yielded an additional 37 raster layers that were used only in Model 2 (the spatial version).

## 2.4 Modelling

150 Till geochemistry data and all rasters were loaded into RStudio using the *terra* package (Hijmans, 2025). The rasters were stacked, and the values were extracted at all till sample locations and added to the till geochemistry data frame. Incomplete observations were removed, producing a dataset of 17,328 samples. The Regional Surficial Geology variable was reclassified to “drift poor” in instances of a till sample falling on bedrock

155 A Random Forest model was constructed to predict the AI% observed in the till samples using the environmental geospatial covariates. The Random Forest algorithm is effective at limiting overfitting, integrating both categorical and numerical data simultaneously, and parsing complex relationships between covariates and response variables, which are desirable characteristics for modelling SOC at a regional scale (Heung et al., 2014; Breiman, 2001). Random Forest is a machine learning approach that uses an ensemble of decision trees to make predictions. Decision trees are grown from randomly selected “bootstrap” samples of the dataset, which each comprise approximately two thirds of the total sample size as a function of sampling with replacement. Decision trees split data observations (i.e., AI%) into increasingly homogenous



groups – at each split assigning a variable ( $m$ ) best explaining the division (Breiman, 2001). This  $m$  is selected from a randomly generated portion ( $mtry$ ) of all total variables ( $M$ ). Predictions are made based on an average of the ensemble, meaning the variables which best explain the AI content are used to make a prediction for each tree, and the average of these forms the final prediction. The samples that were not drawn for each decision tree (i.e., the “out-of-bag” samples) are used to estimate the model accuracy. This built-in validation avoids splitting the dataset into “train” and “validation” partitions during model training. Additionally, 10-fold cross validation was performed to test the model predictions. Finally, Random Forest contains functionality to evaluate relationships between predictor and response variables (i.e., between AI% and environmental variables).

Two models were developed to predict values of AI% across the island of Newfoundland. The Random Forest hyper-parameters for Model 1 were  $M = 7$  (total variables),  $mtry = 4$  (number of variables to draw at each split), and  $ntree = 1000$  (number of trees to grow). Model 2 (the spatial model) used the same covariates as Model 1 but replaced the bedrock geology variable with the 37 individual distance to bedrock geology variables, enabling the model to leverage spatial trends in the geochemistry data. Hyper-parameters for Model 2 were  $M = 44$ ,  $mtry = 13$ , and  $ntree = 2000$ . The  $R^2$  and RMSE were calculated to evaluate each model via out-of-bag cross-validation. The resulting predictions and the predicted standard deviations  $\delta$  of each ensemble model were output as raster layers to visualize spatially the distribution of AI% and model uncertainty, respectively.

## 2.5 Spatial model uncertainty

Following initial modelling and predictions the calibrated uncertainty of the models was derived and mapped spatially to convey confidence in AI predictions. Calibration refers to using the out-of-bag model error to scale  $\delta$  to more realistic values. This is a necessary step to ensure that predicted  $\delta$  reflects known model error, increasing confidence in these predictions. To accomplish calibration of the model uncertainty, the data was split into a test and training set comprising of 10% and 90% of the data respectively, with the training data used to generate calibration values and test data withheld to validate the optimized calibration values. Uncalibrated estimates of uncertainty were extracted from the out-of-bag standard deviation of the predictions of all trees of the Random Forest ensemble. To ascertain whether these estimates of uncertainty required calibration, graphical visual analysis of the training data was first performed (Palmer et al., 2022). The training set was used to generate predictions for both the spatial and aspatial models, and the  $\delta$  of these predictions and the RMSE of residuals were calculated. If the model prediction  $\delta$  accurately represents the uncertainty of predictions, the ratio of the residuals to the  $\delta$  (the  $r$  statistic) should be normally distributed with a standard deviation of 1 (Palmer et al., 2022). The  $r$  statistic was calculated and plotted as a histogram for both models. While this emphasizes the relationship between  $\delta$  and RMSE, it does not conclude whether larger RMSE values correlate with larger  $\delta$  values (Palmer et al., 2022). To evaluate the linear relationship between model  $\delta$  and cross-validated error, the predictions were divided into 15 equal frequency bins by  $\delta$ ,



190 and the RMSE of residuals from each bin is calculated. The RMSE and  $\delta$  are plotted against an identity function and checked for linearity. Preliminary results of both graphical analyses of the training data indicate that while the model uncalibrated standard deviation predictions  $\delta_{UC}$  estimates are fair, they may be improved with calibration.

The Random Forest model prediction uncertainty was thus calibrated according to Palmer et al. (2022), which assumes that the error of predictions – or, residuals  $R(x)$  from the out-of-bag data  $D_{OOB}$  – are linearly related to  $\delta_{UC}$  for any  
 195 given point, or  $\delta_{Cal} = a \delta_{UC}(x) + b$ . Calibration values were obtained by optimizing Eq. (3) using the Nelder-Mead algorithm in R:

$$a, b = \operatorname{argmin}_{a', b'} \sum_{x, y \in D_{OOB}} \ln(2\pi) + \ln((a' \delta_{UC}(x) + b')^2) + \frac{R(x)^2}{(a' \delta_{UC}(x) + b')^2}. \quad (3)$$

This minimizes the negative log likelihood that residuals  $R(x)$  are normally distributed with  $mean = 0$ , and  $SD = a \delta_{UC} + b$  to find optimized values of  $a$  and  $b$  (slope and intercept) that are used to calibrate  $\delta_{UC}$  (uncalibrated standard deviation) via linear model. To validate these results the  $\delta_C$  of the test data were then calculated by scaling  $\delta_{UC}$  by  $a$  and  $b$  using Eq. (4):

200

$$\delta_{Cal} = a \delta_{UC} + b. \quad (4)$$

These were graphically and statistically validated using the same methods detailed above. Following this, the calibration factors were applied to the entire predicted  $\delta$  data and mapped spatially.

### 3 Results

#### 3.1 Mapped predictions and uncertainty

205 Both models predicted high values of Al% in several places throughout the island, notably the Mount Peyton (central northeast), Avalon (most easterly), and Deer Lake (south central west) areas (Fig. 3 a, b). Highs also extend into the southwestern portion of the island, near Port Aux Basques. Low values were predicted in south central Newfoundland, over known weathered sedimentary packages. These patterns were predicted consistently by both models and are not surprising given the geological context. While both models predicted a high Al% near Gros Morne (central western coast), the spatial  
 210 Model 2 predicted high values extending into the Great Northern Peninsula and generally predicted higher values than the aspatial Model 1 in the southwestern area of the island.

The prediction uncertainty  $\delta$  was highest closer to the ocean and with increasing distance from samples – especially on the Great Northern Peninsula (Fig. 3 c, d) where samples are sparse or non-existent (Fig. 1). While this pattern was observed in both outputs, it was more prominent in the spatial model. The aspatial model showed  $\delta$  spread relatively evenly throughout  
 215 the island, with lower values in areas close to samples and areas near the coast or distant from samples showing higher values. Unsurprisingly, bedrock units with few samples also showed a high  $\delta$ .

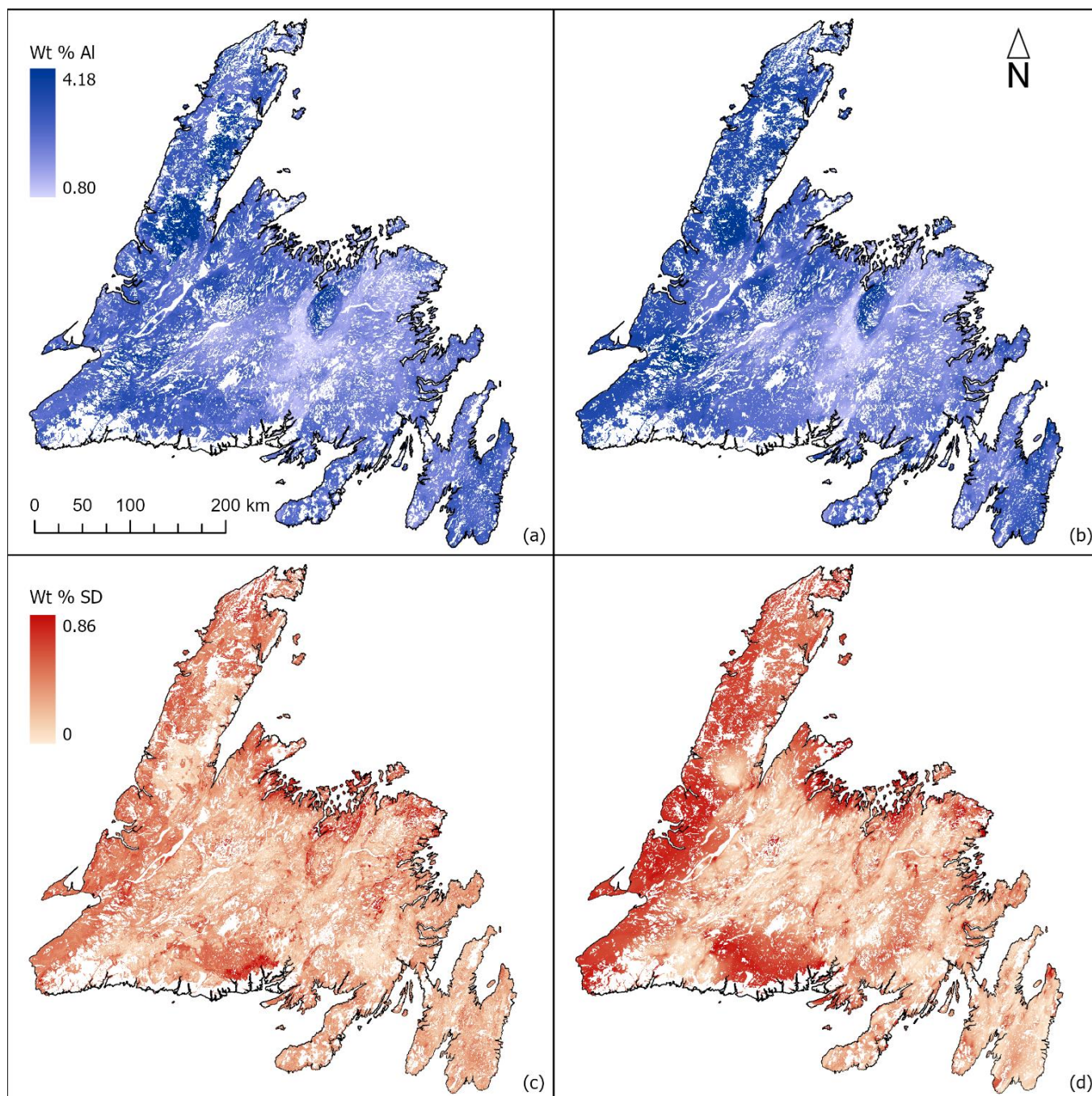


**Figure 3** Aluminum availability (Al%) predictions and corresponding calibrated uncertainty predictions given as Al% (SD) across the island of Newfoundland with aspatial (a, c) and spatial (b, d) models.



## 220 3.2 Uncertainty calibration

Calibrated uncertainty of both models conforms closely to the identity function and the standard normal distribution. Scatterplots or the  $r$  statistic clarified that for both models, uncalibrated points lie beneath the identity function, indicating that both models overestimated  $\delta$ . They also indicated a positive slope between calibrated and uncalibrated values, demonstrating positive correlation between the size of residuals and the size of  $\delta$  estimates. Deviations from this pattern exist – though  
225 primarily in poorly sampled bins (figs. 4 e and f). In both cases, calibration improved the fit of data to both the normal distribution and the identity function. After calibration, normality and accuracy of the  $r$  statistic was improved, with standard deviations calibrated from 0.46 and 0.42 to 1.02 and 1.00, and the RMSE of the  $\delta$  compared to the out-of-bag errors decreased from 0.317 and 0.264 to 0.208 and 0.166 for the aspatial and spatial models respectively – a decrease of approximately 34% and 47%.

230 The uncertainty calibration was most reliable in areas of moderate uncertainty. Figures 4 e and f show the highest uncertainty bin deviating significantly from the identity function, indicating that samples with a calibrated  $\delta$  of greater than approximately 0.22 and 0.25 for the aspatial and spatial models respectively are underestimated. These points represent approximately 7% of samples from both models. Application of the calibration factors to the  $\delta$  rasters translated to 19 % and 40 % of  $\delta$  being underpredicted across Newfoundland aspatially and spatially respectively (fig. 5). These underpredicted areas  
235 coincide entirely with areas of low confidence due to a paucity of samples. This is to be expected; calibrating uncertainty addresses systemic error within model predictions, not error associated with issues in sample distribution. Figures 4 a, b, e, and f clearly demonstrate that overall, the uncertainty calibration corrects the consistent underprediction of  $\delta$  by both models.

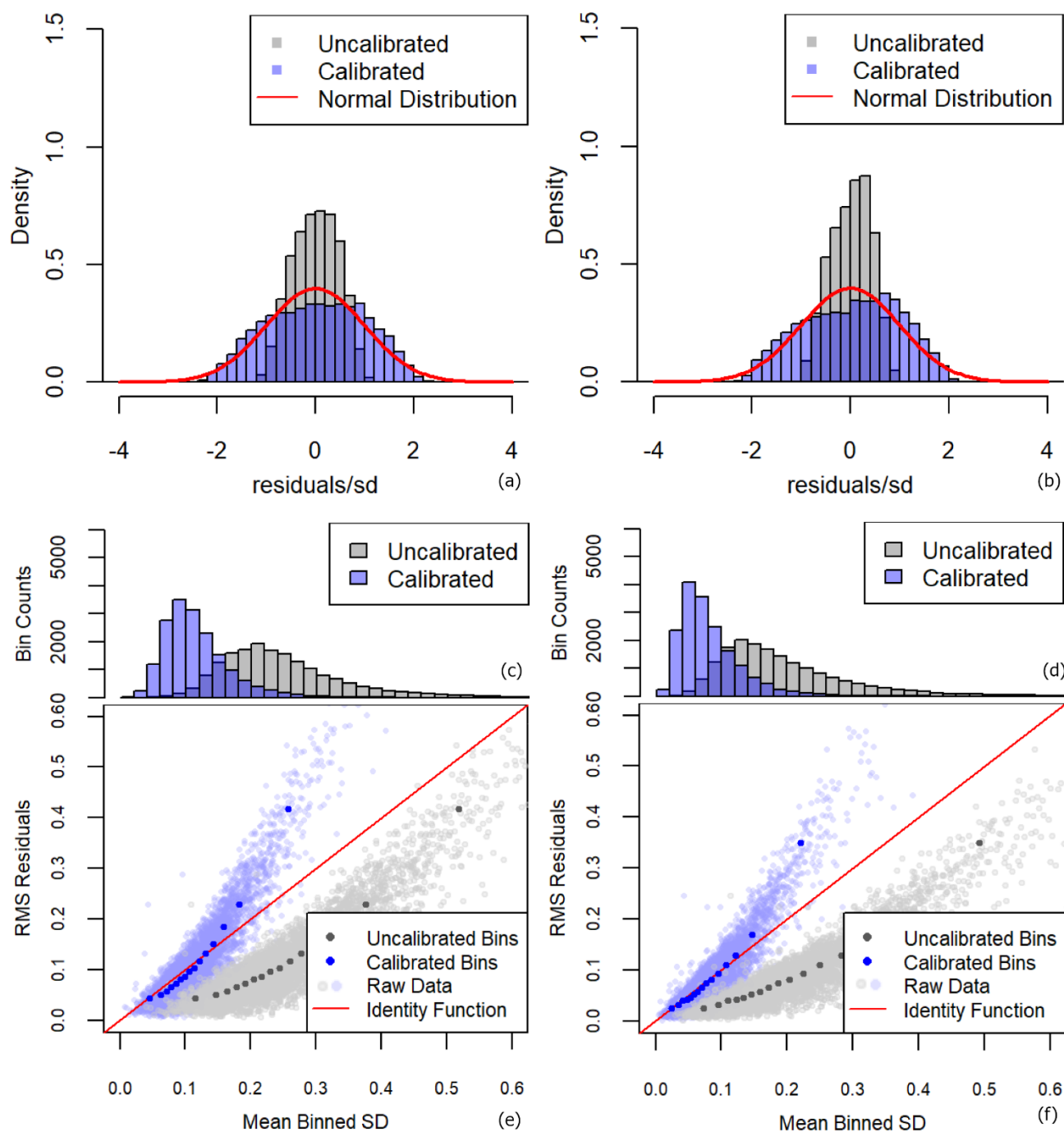


**Figure 4** Distribution of the R statistic (a,b), distribution of sample  $\delta$  (c,d), and residuals vs  $\delta$  plots of both raw data and binned data (e, f) for aspatial (a, c, e) and spatial models (b, d, f).

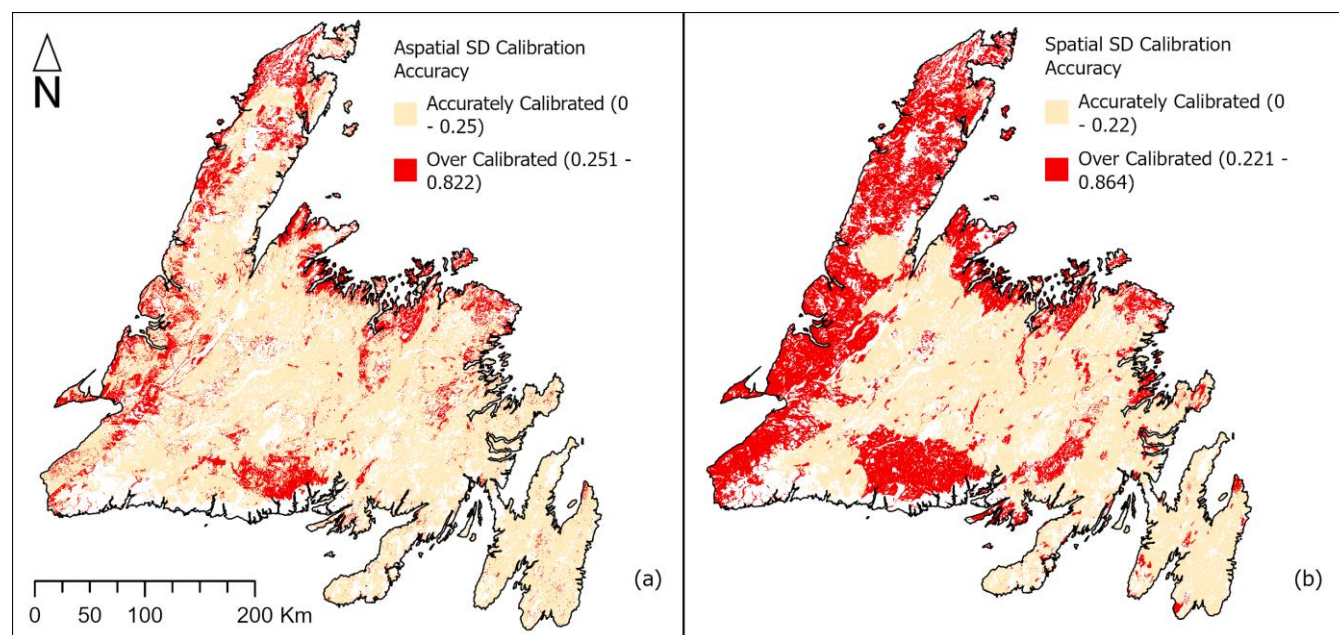


**Figure 5 Map of  $\delta$  calibration accuracy across Newfoundland for aspatial (a) and spatial (b) models.**

### 3.3 Variable importance

Cross-validation demonstrated that Al% in glacial till could be modelled accurately using environmental variables, and with lower uncertainty with the addition of spatial context. The aspatial and spatial models attained R<sup>2</sup> values of 0.59 and 0.71, and RMSE values of 0.34 and 0.29 Al wt% respectively. These results suggest that the spatial model explained >10% more of the variance within sample data than the aspatial model, corresponding to a prediction uncertainty which was lower, on average, by ~0.12 Al wt%.

The most influential variables for the aspatial model were bedrock units, distance from the ocean, elevation, and unit size (see table 2). Climate zone, slope, ruggedness, and surficial deposit type had the least control on Al%. Distance to the ocean was not expected to exert this much influence, and could represent spatial autocorrelation between samples, which motivated the second spatial model (see Methods section). The importance % score of the bedrock variables suggests that while environmental variables can be used to model Al%, the till samples relationship to bedrock and to one another are the most important prediction factors.



Table 2 Aspatial and spatial model variables of importance given as a % of total variance explained.

| Aspatial Model    |                | Spatial Model     |                |
|-------------------|----------------|-------------------|----------------|
| Variable          | Importance (%) | Variable          | Importance (%) |
| Surficial Geology | 4.08           | Surficial Geology | 4.02           |
| Climate           | 4.35           | Climate           | 0.22           |
| Ruggedness        | 7.76           | Ruggedness        | 1.36           |
| Slope             | 7.77           | Slope             | 1.18           |
| Unit Size         | 13.68          | Unit Size         | 1.94           |
| Elevation         | 15.97          | Elevation         | 1.83           |
| Distance to Ocean | 18.23          | Distance to Ocean | 2.16           |
| Bedrock           | 28.14          | Bedrock           | 86.96          |

260 **4 Discussion**

**4.1 Utility of the approach**

Results illustrate the value of mapping and modelling reactive Al using both environmental covariates and spatial context. The resulting map addresses the need to incorporate Al% into SOC modelling in boreal forest mineral soils and to achieve this on a regional scale as informed by Patrick (2022) and recommended by Patrick (2023). This approach has utility in areas where existing soil samples are sparse, but geological information is abundant. Till sampling is widespread due to its applications in mineral exploration, and Al, Ca, Na, and K contents are commonly measured. For example, the GSNL till geochemistry dataset yielded over 17,000 points while the National Soil Network yielded 231 samples in Newfoundland, only 65 of which recorded Al values. Further, when pedogenesis originates from glacial till, soil forms a direct and often indistinguishable boundary with the till. Till samples thus provide an excellent alternative to bedrock maps for soil parent material.

270



## 4.2 Novelty of this work

While previous mapping efforts have addressed the distribution of reactive Al in soils (Ren et al., 2024), this is the first attempt to map it in soil parent material. Support for modelling till geochemistry through existing datasets is likely more common than reactive Al in soil, as demonstrated in Newfoundland, with potential for providing a key factor supporting SOC  
275 modelling across more regions. Few studies investigate till geochemistry from a predictive geochemical standpoint, and those that do focus on economically viable trace elements such as rare earth elements (e.g. Casey et al., 2024). The results developed from this model can be used directly in future SOC models in Newfoundland and provides an important demonstration relevant to the development of SOC modelling in other boreal regions.

The uncertainty calibration is an uncommon yet important component to this project. Addressing uncertainty in SOC  
280 modelling has been identified as essential (Mishra et al., 2013); however, while many digital soil mapping studies produce spatial predictions (Pouladi et al., 2023) few provide spatial estimates of uncertainty, and even fewer provide calibrated uncertainty estimates. The calibration step may be critical for accurately reporting model uncertainty; here, calibration improved uncertainty estimates by over 30% in both cases. These calibrated estimates of uncertainty are critical for operationalizing these results to accurately constrain estimates of SOC stocks. An accurate spatial representation of uncertainty  
285 indicates regions of the study area that are predicted with lower confidence, which could be a) integrated into subsequent models or calculations of SOC stock for the island of Newfoundland, or b) used to guide future sampling to improve spatial estimates of Al%.

## 4.3 Limitations

Several constraints limit these models. While our results indicate bedrock geology is the largest control on Al%,  
290 generally, there is a lack of understanding as to what variables, or interactions between variables, exactly control Al weathering within glacial till. For example, biotic factors, which have been shown to influence soil Al% at coarser scales (Ren et al., 2024), were not explored for the purpose of this study. Further, the model used geological context to leverage spatial autocorrelation within the samples, mimicking a geostatistical approach. While this improved model performance, it renders  
295 partial dependence plots for the spatial model difficult to interpret, and the individual variables difficult to rank. Finally, because the work was focused strongly on spatial predictive accuracy, multicollinearity was left largely unaddressed, making it possible that variable importance was split across multiple correlated predictor variables. Such limitations mean that this modelling approach is less useful for discerning strong predictors for reactive Al content in glacial till but rather is a useful approach for obtaining a spatial prediction for reactive Al in soil parent material. This represents a first order component for  
300 predictive modelling of boreal forest SOC. Next steps, however, should focus on assessing predictors of the relationship between reactive Al in parent material and the overlying boreal forest mineral soil including biotic topographic, and climatic factors and their interactions (Brantley et al., 2017; Maher, 2010, Patrick 2023).



#### 4.4 Utility of the spatial and aspatial models

The patterns of uncertainty across the spatial and aspatial models indicate that the spatial model may be more useful in previously sampled areas, while the aspatial model may deliver higher certainty in areas with scarce samples. While the overall accuracy of the aspatial model is lower, uncertainty is distributed more evenly across space than the spatial model. As seen in figs. 4 and 5 the calibration accuracy is slightly higher in the spatial model than the aspatial model. It may be possible to aggregate both models for regional scale mapping, while for finer scale mapping the model with higher local performance will be preferred.

#### 4.5 Future work

Soil geochemistry is controlled largely by parent material – in this case till – and this in turn controls the ability of soils formed to store C. For example, reactive Al content of soil is a key factor controlling SOC content of boreal forest podzols in the study region (Patrick et al. 2022). The exact nature of the relationship between till and soil geochemistry is not fully understood, however, topography and climate likely play key interacting roles. To inform this relationship, soil and till should be sampled simultaneously at sites informed by this predictive model. Specifically, sampling where there is forecasted high or very low Al, as these extremes may best illustrate the relationships between soil Al% and till Al%. Sampling should be conducted on similar slopes to ensure that the relationship between till and soil is being captured without influence from terrain characteristics, where higher slope areas experience less vertical and more lateral flow resulting in a shallower horizon of SOC enrichment (Patrick, 2023). As depth of horizon is strongly correlated to other soil characteristics governing SOC storage and this may cause variations in SOC content not attributable to parent material alone (Patrick, 2023). Sampling on high and low slopes should then also proceed to assess controls of terrain on SOC storage.

The GSNL continually updates their till sample geochemistry database and new samples should be incorporated as they become available. Till samples from western Newfoundland, particularly the Great Northern Peninsula, will be especially valuable. Additionally, independent glacial till sampling should be prioritized in high uncertainty areas to increase the robustness of these models.

Given the important role that parent material plays in regulating SOC (Slessarev et al.; Patrick et al. 2022) increased attention must be given to improving parent material composition estimates for SOC modelling. This includes further investigation into key parameters controlling Al weathering and thus reactive Al in parent material. The results of the calibration in this study demonstrate the advantages of uncertainty quantification. Future SOC modelling should incorporate this dimension, as should any future mapping of parent material, as it is crucial to producing meaningful model predictions. In the case of modelling SOC, the more reliable the uncertainty the clearer the utility of the predictions for future model development or application for mitigation efforts.



## 5 Conclusion

Using both a spatial and aspatial approach, reactive Al% was successfully modelled and mapped in soil parent material across the Island of Newfoundland for the first time at a high resolution. Calibrated uncertainty was also estimated, providing spatial estimates of model confidence throughout the study area. There is broad utility in predicting parent material geochemistry because it is known to influence soil properties and it draws on a sample base much wider, in many cases, than available soil samples. While future research may expand the sample distribution, and explore relationship between glacial till and soil geochemistry, this work provides a critical component for a future mechanistic SOC model tailored to the soils of Newfoundland and Labrador. This will enable further investigation of the performance of previous modelling across various landscapes, topographies, and soil Al% delivering valuable insight into the spatial distribution of boreal forest SOC across the island. By enabling continuous predictions of SOC and better estimates of the terrestrial carbon reservoir in Newfoundland, this future work will provide a template for such research in other boreal regions.

345



### **Code Availability**

Code developed for both modelling available AI and calibrating uncertainty are publicly available at <https://doi.org/10.5281/zenodo.16109126>.

### 350 **Data Availability**

All raster files, the till geochemistry shapefile, and key results are available at <https://doi.org/10.5683/SP3/6AONRU>.

### **Author Contributions**

SMQ compiled the data, contributed to methodology, performed data analyses, validated the research outputs, visualized the data, interpreted findings, and prepared the original draft of the manuscript. MEP conceptualized and designed the project and  
355 initially supervised the research. BM contributed to coding and methodology, interpreted findings, supervised all aspects of the research, and reviewed and edited the manuscript. SEZ conceptualized the study, interpreted findings, supervised all aspects of the research, and reviewed and edited the manuscript.

### **Competing Interests**

The authors declare they have no competing interests.

### 360 **Acknowledgements**

The authors gratefully acknowledge the insight, support, and advice of Heather Campbell of the Quaternary section of the GSNL as it pertains to details of till geochemistry and navigating the GSNL till geochemistry dataset.

### **Financial Support**

365 This research has been supported by the Canada Research Chairs and National Sciences and Engineering Research Council of Canada Discovery Grants (RGPIN-2018-05383 and RGPIN-2025-07219) programs.



## References

- Adhikari, K., Mishra, U., Owens, P. R., Libohova, Z., Wills, S. A., Riley, W. J., Hoffman, F. M., & Smith, D. R.: Importance  
 370 and strength of environmental controllers of soil organic carbon changes with scale, *Geoderma*, 375, p.114472.  
<https://doi.org/10.1016/j.geoderma.2020.114472>, 2020.
- Ameray, A., Bergeron, Y., Valeria, O. et al.: Forest Carbon Management: a Review of Silvicultural Practices and Management  
 Strategies Across Boreal, Temperate and Tropical Forests, *Curr Forestry Rep* 7, 245–266,  
<https://doi.org/10.1007/s40725-021-00151-w>, 2021.
- 375 Baldock, J.A., Skjemstad, J.O.: Role of the soil matrix and minerals in protecting natural organic materials against biological  
 attack, *Org Geochem* 31, 697–710, [https://doi.org/10.1016/S0146-6380\(00\)00049-8](https://doi.org/10.1016/S0146-6380(00)00049-8), 2000.
- Brantley, S. L., Eissenstat, D. M., Marshall, J. A., Godsey, S. E., Balogh-Brunstad, Z., Karwan, D. L., Papuga, S. A., Roering,  
 J., Dawson, T. E., Evaristo, J., Chadwick, O., McDonnell, J. J., & Weathers, K. C.: Reviews and syntheses: on the  
 roles trees play in building and plumbing the critical zone, *Biogeosciences*, 14, 5115–5142,  
 380 <https://doi.org/10.5194/bg-14-5115-2017>, 2017.
- Breiman, L.: Random Forests, *Machine Learning*, 45, 5–32 <https://doi.org/10.1023/A:1010933404324>, 2001.
- Casey, P., Morris, G., & Sadeghi, M.: Derivation of Predictive Layers Using Regional Till Geochemistry Data for Mineral  
 Potential Mapping of the REE Line of Bergslagen, Central Sweden, *Minerals (Basel)*, 14, 753–.  
<https://doi.org/10.3390/min14080753>, 2024.
- 385 Crowther, T. W., Todd-Brown, K. E. O., Rowe, C. W., Wieder, W. R., Carey, J. C., Machmuller, M. B., Snoek, B. L., Fang,  
 S., Zhou, G., Allison, S. D., Blair, J. M., Bridgham, S. D., Burton, A. J., Carrillo, Y., Reich, P. B., Clark, J. S., Classen,  
 A. T., Dijkstra, F. A., Elberling, B., Bradford, M. A.: Quantifying global soil carbon losses in response to warming,  
*Nature (London)*, 540, 104–108, <https://doi.org/10.1038/nature20150>, 2016.
- Deluca, T. H., Boisvenue, C.: Boreal forest soil carbon: distribution, function and modelling, *Forestry: An International Journal*  
 390 *of Forest Research*, 85, 161–184, <https://doi.org/10.1093/forestry/cps003>, 2012.
- Fick, S.E. and Hijmans, R.J.: WorldClim 2: new 1 km spatial resolution climate surfaces for global land areas, *International*  
*Journal of Climatology*, 37, 4302–4315, 2017
- Friedlingstein, P., Meinshausen, M., Arora, V.K., Jones, C.D., Anav, A., Liddicoat, S.K., Knutti, R.: Uncertainties in CMIP5  
 climate projections due to carbon cycle feedbacks, *J Clim* 27, 511–526, <https://doi.org/10.1175/JCLI-D-12-00579.1>,  
 395 2014.
- Government of Canada, HRDEM, <https://open.canada.ca/data/en/dataset/957782bf-847c-4644-a757-e383c0057995>, 2024.
- Government of Newfoundland and Labrador Fisheries, Forestry, and Agriculture, NLDEM, <https://geohub-gnl.hub.arcgis.com/maps/7203aef91a024ece843c4be4b3727dda/about>, 2023.



- Heung, B., Bulmer, C. E., & Schmidt, M. G.: Predictive soil parent material mapping at a regional-scale; a Random Forest  
 400 approach, *Geoderma*, 214–215, 141–154, <https://doi.org/10.1016/j.geoderma.2013.09.016>, 2014.
- Hijmans, R.: terra: Spatial Data Analysis, R package version 1.8-2, <https://CRAN.R-project.org/package=terra>, 2025.
- Hillier, J., Brentrup, F., Wattenbach, M., Walter, C., Garcia-Suarez, T., Mila-i-Canals, L., & Smith, P.: Which cropland  
 greenhouse gas mitigation options give the greatest benefits in different world regions? Climate and soil-specific  
 predictions from integrated empirical models, *Global Change Biology*, 18, 1880–1894,  
 405 <https://doi.org/10.1111/j.1365-2486.2012.02671.x>, 2012.
- Hagemann, U., Moroni, M. T., Shaw, C. H., Kurz, W. A., & Makeschin, F.: Comparing measured and modelled forest carbon  
 stocks in high-boreal forests of harvest and natural-disturbance origin in Labrador, Canada, *Ecological Modelling*,  
 221, 825–839, <https://doi.org/10.1016/j.ecolmodel.2009.11.024>, 2010.
- Ilich, A. R., Misiuk, B., Lecours, V., & Murawski, S. A.: MultiscaleDTM: An open-source R package for multiscale  
 410 geomorphometric analysis, *Transactions in GIS*, 27, 1164–1204, <https://doi.org/10.1111/tgis.13067>, 2023.
- Jackson, R.B., Lajtha, K., Crow, S.E., Hugelius, G., Kramer, M.G. and Pineiro, G.: The ecology of soil carbon: Pools,  
 vulnerabilities, and biotic and biotic controls, *ANNU REV ECOL EVOL S* 48, 419–45, 2017.
- Jenny, H., Gessel, S. P., & Bingham, F. T. (1949). Comparative study of decomposition rates of organic matter in temperate  
 and tropical regions. *Soil Science*, 68, 419–432. <https://doi.org/10.1097/00010694-194912000-00001>
- 415 Lawley, R., Smith, B., de Lourdes Mendonca-Santos, M., Hartemink, A. E., McBratney, A. B., McBratney, A., Mendonça-  
 Santos, M. de L., & Hartemink, A. E.: Digital soil mapping at a national scale; a knowledge and GIS based approach  
 to improving parent material and property information, In *Digital Soil Mapping with Limited Data*, 173–182,  
[https://doi.org/10.1007/978-1-4020-8592-5\\_14](https://doi.org/10.1007/978-1-4020-8592-5_14), 2008.
- Maher, K.: The dependence of chemical weathering rates on fluid residence time, *Earth and Planetary Science Letters*, 294,  
 420 101–110, <https://doi.org/10.1016/j.epsl.2010.03.010>, 2010.
- McNally, A., NASA/GSFC/HSL: FLDAS Noah Land Surface Model L4 Global Monthly 0.1 x 0.1 degree (MERRA-2 and  
 CHIRPS), Greenbelt, MD, USA, Goddard Earth Sciences Data and Information Services Center (GES DISC),  
 10.5067/5NHC22T9375G, 2018.
- McNicol, G., Bulmer, C., D’Amore, D., Sanborn, P., Saunders, S., Giesbrecht, I., Arriola, S. G., Bidlack, A., Butman, D., &  
 425 Buma, B.: Large, climate-sensitive soil carbon stocks mapped with pedology-informed machine learning in the North  
 Pacific coastal temperate rainforest, *Environmental Research Letters*, 14, 14004-, <https://doi.org/10.1088/1748-9326/aaed52>, 2019.
- Mishra, U., Jastrow, J. D., Matamala, R., Hugelius, G., Koven, C. D., Harden, J. W., Ping, C. L., Michaelson, G. J., Fan, Z.,  
 Miller, R. M., McGuire, A. D., Tarnocai, C., Kuhry, P., Riley, W. J., Schaefer, K., Schuur, E. A. G., Jorgenson, M.  
 430 T., & Hinzman, L. D.: Empirical estimates to reduce modeling uncertainties of soil organic carbon in permafrost  
 regions; a review of recent progress and remaining challenges, *Environmental Research Letters*, 8, 035020,  
<https://doi.org/10.1088/1748-9326/8/3/035020>, 2013.



- Nesbitt, H. W., & Young, G. M.: Prediction of some weathering trends of plutonic and volcanic rocks based on thermodynamic and kinetic considerations, *Geochimica et Cosmochimica Acta*, 48, 1523–1534, [https://doi.org/10.1016/0016-7037\(84\)90408-3](https://doi.org/10.1016/0016-7037(84)90408-3), 1984.
- Newfoundland and Labrador Geological Survey, Till Geochemistry, Newfoundland and Labrador GeoScience Atlas OnLine [dataset], <https://geoatlas.gov.nl.ca/>, 2024.
- Oades, J. M.: The retention of organic matter in soils, *Biogeochemistry*, 5, 35–70, <https://doi.org/10.1007/BF02180317>, 1988.
- Palmer, G., Du, S., Politowicz, A., Emory, J. P., Yang, X., Gautam, A., Gupta, G., Li, Z., Jacobs, R., & Morgan, D.: Calibration after bootstrap for accurate uncertainty quantification in regression models, *Npj Computational Materials*, 8, Article 115, <https://doi.org/10.1038/s41524-022-00794-8>, 2022.
- Paré, D., Bognounou, F., Emilson, E. J. S., Laganière, J., Leach, J., Mansuy, N., Martineau, C., Norris, C., Venier, L., & Webster, K.: Connecting forest soil properties with ecosystem services: Toward a better use of digital soil maps—A review, *Soil Science Society of America Journal*, 88, 981–999, <https://doi.org/10.1002/saj2.20705>, 2024.
- Patrick, M. E., Young, C. T., Zimmerman, A. R., & Ziegler, S. E.: Mineralogic controls are harbingers of hydrological controls on soil organic matter content in warmer boreal forests, *Geoderma*, 425, Article 116059, <https://doi.org/10.1016/j.geoderma.2022.116059>, 2022.
- Patrick, M.E.: The roles of parent material, climate, and geomorphology in soil organic carbon response to short-term climate change in moist boreal forests, Doctor of Philosophy Dissertation, Department of Earth Sciences, Memorial University of Newfoundland, pp 265, <https://doi.org/10.48336/SKF9-1132> 2023, .
- Pierson, D., Lohse, K. A., Wieder, W. R., Patton, N. R., Facer, J., de Graaff, M.-A., Georgiou, K., Seyfried, M. S., Flerchinger, G., & Will, R.: Optimizing process-based models to predict current and future soil organic carbon stocks at high-resolution, *Scientific Reports*, 12, 10824–10824, <https://doi.org/10.1038/s41598-022-14224-8>, 2022.
- Pouladi, N., Gholizadeh, A., Khosravi, V., & Boruvka, L.: Digital mapping of soil organic carbon using remote sensing data; a systematic review, *Catena (Giessen)*, 232, 107409-, <https://doi.org/10.1016/j.catena.2023.107409>, 2023.
- Quinn, S. M., Misiuk, B., Ziegler, S., Patrick, M.: Replication Data for: Mapping and modelling a boreal forest soil organic carbon predictor in the glacial till of Newfoundland, Canada, Memorial University Dataverse (Borealis) [dataset], <https://doi.org/10.5683/SP3/6AONRU>, 2025.
- Quinn, S. M., Misiuk, B., Ziegler, S., Patrick, M.: SMQuinn\_Mapping\_and\_modelling\_a\_boreal\_forest\_soil\_organic\_carbon\_predictor\_in\_glacial\_tills\_of\_NL, Zenodo [code], <https://doi.org/10.5281/zenodo.16109126>, 2025.
- Rasmussen, C., Heckman, K., Wieder, W. R., Keiluweit, M., Lawrence, C. R., Berhe, A. A., Blankinship, J. C., Crow, S. E., Druhan, J. L., Hicks Pries, C. E., Marin-Spiotta, E., Plante, A. F., Schädel, C., Schimel, J. P., Sierra, C. A., Thompson, A., & Wagai, R.: Beyond clay: Towards an improved set of variables for predicting soil organic matter content, *Biogeochemistry*, 137, 297–306. <https://doi.org/10.1007/s10533-018-0424-3>, 2018.



- Ren, S., Wang, C., & Zhou, Z., Global Distributions of Reactive Iron and Aluminum Influence the Spatial Variation of Soil Organic Carbon, *Global Change Biology*, 30, e17576-n/a., <https://doi.org/10.1111/gcb.17576>, 2024.
- Scharlemann, J. P., Tanner, E. V., Hiederer, R., Kapos, V.: Global soil carbon: understanding and managing the largest terrestrial carbon pool, *Carbon Management*, 5, 81-91, <https://doi.org/10.4155/cmt.13.77>, 2014.
- 470 Slessarev, E.W., Chadwick, O.A., Sokol, N.W., Nuccio, E.E., Pett-Ridge, J.: Rock weathering controls the potential for soil carbon storage at a continental scale, *Biogeochemistry* 157, 1-13, <https://doi.org/10.1007/s10533-021-00859-8>, 2022.
- Wang, L.: Assessment of land use change and carbon emission: A Log Mean Divisa (LMDI) approach, *Heliyon*, 10, e25669 <https://doi.org/10.1016/j.heliyon.2024.e25669>, 2024.
- Wang, X., Wackett, A.A., Toner, B.M., Yoo, K.: Consistent mineral-associated organic carbon chemistry with variable erosion  
 475 rates in a mountainous landscape, *Geoderma*, 405, <https://doi.org/10.1016/j.geoderma.2021.115448>, 2022.
- Zhang, H., Goll, D. S., Wang, Y., Ciais, P., Wieder, W. R., Abramoff, R., Huang, Y., Guenet, B., Prescher, A., Viscarra Rossel, R. A., Barré, P., Chenu, C., Zhou, G., & Tang, X.: Microbial dynamics and soil physicochemical properties explain large-scale variations in soil organic carbon, *Global Change Biology*, 26, <https://doi.org/10.1111/gcb.14994>, 2020.
- Zhou, Z., Ren, C., Wang, C., Delgado-Baquerizo, M., Luo, Y., Luo, Z., Du, Z., Zhu, B., Yang, Y., Jiao, S., Zhao, F., Cai, A.,  
 480 Yang, G., & Wei, G.: Global turnover of soil mineral-associated and particulate organic carbon, *Nature Communications*, 15, <https://doi.org/10.1038/s41467-024-49743-7>, 2024.